Magnetic Circuit & Torque Analysis Of Brushless DC Motor

Dr. Arif J. Abass   **Mohamed Rashide**   **Kais Wadi**
Lecturer   **Assist. Lecturer**   **Assist. Lecturer**
Electrical Engineering Dept., Engineering College

Abstract
This work is concerned with magnetic and torque analysis of BLDCM and with development of a method of designing BLDCM that have symmetric winding on the rotor .make significant contribution to the rotor inductance position difficult. It is also show that the prediction detent torque can be extremely sensitive to the permanent magnet by altering magnet arc width. Finally, simple lumped models that allow one to predict motor performance and characteristics as a function of main dimension, magnet residual flux density and phase current are developed. These models are used as a basis for an approach to designing BLDCM
Keywords: Rotor construction: Armature windings, Equivalent circuit, Torque analysis.

تحليل العزم المغناطيسي لمحرك التيار المستمر بدون فرش انزلاق

الخلاصة:
يتناول هذا البحث بصورة مركزة دراسة المغناطيسية والتحليل لعزم محرك التيار المستمر بدون فرش انزلاق وإمكانية إجراء عمليات تطويرية لطريقة تصميم هذا المحرك الذي يحتوي على ملفات متماثلة لعضو الدوار والتي هي ذات أهمية عالية لتحديد وضعية العضو الدوار نسبة إلى الحث المغناطيسي المؤثر عليه .

لوحظ أيضا أن العزم السلبي يؤثر بحساسية عالية على المغناطيس الدائمي المتكون منه هذا المحرك، عند إجراء تعديلات على عرض القوس المغناطيسي. وأخيرا تم اخذ طراز نوع من المحرك هـذا لإجراء دراسـة عليه والتي شملت الأداء والخصائص كدالة اللابعاد الرئيسية له وكثافة الحث المغناطيسي المتولد الذي لـه تأثير سلبـي وكذلك تأثير طور التيار .إن هذه الأنواع من المحركات التي تـم دراستها استخدمت كأساس لتعممحركات التيار المستمر بدون فرش.

Notations

B_g	Air-gap flux density
e	Instantaneous e.m.f. induced in coil
e_p	Per-phase r.m.s e.m.f.
E_a	Stator generated voltage
I_{dc}	Stator (armature) current (same as dc bus current)
l	Length of the stator
I_a	Armature current
K_t	Motor 's torque constant (Nm/A)
L_1	Conventional leakage inductance

per phase

L_{zz}	Normal zigzag leakage Inductance
L_p	Peripheral air gap leakage Inductance
N_C	Total number of current carrying conductors
N_p	Turns per pole
p	Number of pole pairs

Notations
P Power
R Sum of the individual phase

resistance

R_a/r_a Stator resistance per phase

T_e Electric Mechanical torque output

V_t Applied terminal voltage

ψ_{max} Total flux linkage

$\psi(\theta)$ Flux linkage considered to rotor position θ

ω_m Mechanical rotational speed in rad s^{-1}.

Latin symbols

θ   Angle of rotor position

Introduction

Brushless dc motors are typically configured as permanent magnet motors with electronic circuit to supply power to each of the stator winding phases in synchronism with the rotor angular position. The motor drive electronics usually derive power from a dc power bus and the field is supplied by a rotating permanent magnet configuration without a wound field or brushes. In many applications, a front-end rectifier is built into the same electronics package as the motor control to take power from an ac source.

The advantage of brushless dc motors lies in the absence of rotating contacts such as slip ring brushes in the case of conventional wound-field synchronous motors, or commutating brushes in the case of conventional commutator's type dc motors. The absence of brushes eliminates the periodic inspection and maintenance required as in this brush-type motor. The brushless dc motor, however, requires rotor position sensing, and that the magnets to be firmly restrained on the rotor structure, and lacks field control (motor back-emf is a function of speed only, and is affected by magnet temperature and armature winding mmf).

In spite of these disadvantages, the brushless permanent magnet motor is gaining increasing use because of its low maintenance and the availability of inexpensive and robust power electronics for motor control. [1] .

Rotor Construction

The simplest form of brushless dc motor rotor construction uses a cylindrical shaft and a ferromagnetic rotating structure with a surface on which magnets are fixed. The magnets are radially magnetized and the magnet outer surfaces are ground or preformed to be concentric with the stator inside diameter.

The magnets are held in place by a structural adhesive to prevent radial movement during operation. The inner magnetic structure is machined round or with an even number of flat surfaces around the periphery to accept magnets with matching inner surfaces. This structure may suffice for many applications where the motor is small (usually fractional horsepower ratings) and the maximum operating or over speed, rating is low enough to prevent structural failure of the rotor.

This simple surface mount construction helps to keep motor costs down, but the cost of rotor failure can be high when the stator or connected shaft load is damaged, or an unsafe condition results from rotor failure. Figure (1) and Figure (2) show two 6-pole and 4-pole brushless dc rotor cross sections with two different magnet mounting surface configurations. The magnet polarity, designated by N or S, alternates around the periphery. The figures also show a magnet containment band on each rotor surface [2]. The rotor design and be as follows:-

a - Sleeved Rotors

In high-speed integral horsepower motors, there are several ways to retain the permanent magnets without significant loss of motor performance. One of the most popular is a thin steel sleeve shrunk on the rotor surface over the magnet outside diameter (see Figs. (1) and(2)). The steel is high strength and can be stainless non-magnetic or magnetic steel.

For a magnetic steel sleeve, the sleeve will divert a very small portion of the magnetic flux away from the air gap to the adjacent opposite-polarity magnet, but the performance loss is small because of the steel saturation and small radial dimension of the sleeve. In this construction method, the hoop strength of the sleeve is relied on to prevent the magnets from lifting off the rotor structure at the maximum rotor over speed condition [2].

b -Banded Rotors

Another method is adhesive-impregnated glass tape, carbon fiber, or other high-strength fiber banding. The banding is wound around the rotor under tension after the magnets have been assembled on the rotor surface.

The tension is calculated to be enough to prevent the magnets from lifting off the mounting surface at the highest over speed condition. The adhesive is cured in an oven and relied on to hold the fibers together during all modes of operating temperature and speed. This method works well where there are no sharp magnet corners or edges on the rotor surface to cause a stress concentration in the high-strength fiber banding [2].

c - Buried Permanent Magnets

An additional means of construction to ensure rotor integrity is the buried magnet configuration in which the magnets are inserted into axial slots in a laminated rotor structure. Small storable bridges are used to provide a continuous outer cylinder for tensile strength, while various nonmagnetic openings are punched in the laminations to provide tangential flux baffles. In some designs, these rotor configurations have aluminum cast into the rotor for line starting from an ac supply, and are not used as brushless dc motors [3].

Rotor position sensors are necessary for precision brushless D.C. motor control, and these sensors must be mechanically and electrically identical for all operating conditions to provide a highly reliable drive system. Rotor position sensing may be performed optically, magnetically, or by some other means to send rotor position information to a stationary controller without brushes or other rotating contacts. These types of sensing devices tend to reduce motor reliability, and care must be taken to provide a robust rotor position sensing method [4].

A variety of magnet materials is available to provide the required rotating magnetic field in a brushless dc motor. The most popular are ceramic ferrite, samarium-cobalt, and neodymium-iron-boron magnets. Alnico rotating magnetic field in a brushless dc motor. The most popular are ceramic ferrite, samarium-cobalt, and neodymium-iron-boron magnets. Alnico magnets, once very popular, are not used extensively in brushless dc motors because of their poor demagnetization resistance. Ferrites are the least expensive, but have a low B-H characteristic, and require a thick magnet to obtain a reasonable air-gap magnetic flux density[5].

Samarium-cobalt magnets are expensive, but have a high B-H characteristic and a high Curie temperature and thus a high operating

temperature capability. Neodymium-iron boron magnets are expensive but have the highest B-H characteristic. The Curie and operating temperatures are lower than for samarium-cobalt magnets. The magnetic properties are characterized by a B-H curve showing the basic demagnetization properties of the material independent of the magnetic circuit in which it will be used.

This B-H curve is a second-quadrant plot of magnet flux density (B) vs. magneto-motive force per unit length (H). Figure (3) shows a B-H plot for several magnet material types. Because of the large number of magnet characteristics available within each of the four family types shown in Fig. (3), the curves show only gross characteristics for each magnet family, and not for a specific member of the family. The units used on the two axes are teslas (webers per square meter) for flux density and kiloampere-turns per meter for magnetomotive force per unit length [6].

Armature Windings and Equivalent Circuit

A number of stationary winding types may be used for brushless dc motors, including two-phase and three-phase concentric and distributed windings that are supplied with power from electronic controllers. The electronic controllers require some form of rotor position feedback for switching power among the phase windings so that the stator (armature) currents follow the rotor to produce a torque in synchronism with the rotor speed. Most large brushless dc motors utilize a three-phase distributed stator winding that is wound in 60- degree phase belts with two coil sides per slot. This section covers, the characteristics of this conventional three-phase winding type and its associated effects on the magnet and torque production. Figure (4) shows a

representation of the phase belt locations inside the stator core where the stator slots are located for a two-pole, three-phase, two-layer, full-pitch winding [7].

In this winding for a two-pole motor, there are two coil sides per slot and each coil spans 180 degrees, mechanical as well as electrical. This winding, with the current-carrying conductors located directly in the magnetic flux created by the rotor magnets, produces an mmf that adds to one-half of the rotor magnet mmf and subtracts from the other half of the rotor magnet mmf. On average, without saturation, the total demagnetization effect is near zero. However, in the portion of the magnetic field enhanced by the stator mmf, stator tooth density may be driven further into saturation, and the total ampere turns required to drive the magnetic flux into the stator is increased in a nonlinear fashion that changes the operating point of the magnet as shown in Fig. (5).

Because of an effect it is difficult to determine without a magnetic field analysis, the usual value of 10% of the total stator (armature) mmf for conventional dc machines can be assumed as the additional amount of ampere-turns required to be supplied by the magnet under load conditions. The approximate value to be used for armature mmf demagnetization is:

$$AMMF_m = 0.1 I_{dc} N_c / (2P) \quad ....(1)$$
where:

N_c = 2/3 (Slots) (coil sides per slot)(turns per coil)/circuits

The 2/3 in the equation for Nc is for the fact that only two of the 3 phases are conducting current at a time for 120-degree conduction.

Figure (6) shows the phase belt locations for a fractional pitch winding. In this winding for a two-pole motor, each coil side spans less than 180

degrees, and while producing slightly less back-emf, results in smaller end turns and a more distributed mmf. A short-pitched winding is more typical of ac synchronous and induction machines to produce a more sinusoidal stator mmf. For the brushless dc motor, the use of a short-pitched winding reduces some of the torque pulsations resulting from the electronic commutation of the stator phases.

The stator winding mmf is concentrated at the coil sides carrying current, and the rotor torque is developed from the interaction of the rotor magnetic flux and the stator currents. In a conventional dc motor, the load angle is approximately 90 electrical degrees because the stator coils are commutated one at a time, and the brush position is such that the armature coils carrying current are in the maximum dc field flux virtually all the time. A brushless dc motor controller, however, switches a large portion of the winding every 60 electrical degrees and the current carrying stator conductors are not always centered with respect to the rotor magnetic flux. For this reason, some reduction of the winding effectiveness results, and must be considered in the design process[8].

The equivalent circuit for a brushless dc motor consists of a dc source, a series resistance, and a generated voltage that opposes the source voltage. Because the brushless dc motor as shown in Fig.(7) is a variable speed device, the input voltage must be controlled to match current and voltage to the desired load and speed. The applied motor terminal voltage is given by:

$$V_t = E_a + I_{dc} 2R_a \ldots\ldots\ldots\ldots\ldots\ldots (2)$$

The voltage Vt is the steady-state voltage applied directly to the motor terminals by the electronic motor controller, and is controlled to give the desired torque and speed in response to some desired steady-state motor performance point. For transient performance, a series inductance should be included in the equivalent series circuit. The inductance would be the modified leakage inductance for two stator phases in series, because the typical brushless dc motor has magnets only on the rotor, and no surface iron structure, the zigzag component of leakage inductance should be eliminated from the calculation, and the peripheral component should be included since the equivalent total air gap includes the magnet thickness. The equivalent stator leakage inductance per phase is:

$$L_{1e} = L_1 L_{ZZ} + L_p \ldots\ldots\ldots\ldots\ldots\ldots (3)$$

Torque Analysis

The basic torque and voltage equations of d.c. brushless motors closely resemble those of D.C. brushed motors. A simple analysis for determining a motor's characteristics; this also allows an appreciation of its limitations. In this analysis, a simple two-pole motor is considered (see Figure (8), the key features of this design are the rotor's magnetic pole arc of 180°, and a three-phase stator winding with two slots per phase and N turns per slot. The air-gap flux, neglecting any fringing, can be considered to be a square wave (see Figure 9(a)).

As the rotor is rotated, a voltage is induced within the stator windings, and the flux linkage varies linearly as a function of the rotor position, with the maximum positive linkage for the winding occurring at θ = 0° and the maximum negative flux linkage occurring at θ = 180° [9].

If a single phase is considered, the total flux linkage can be determined by integrating the contribution of

individual turns, to give a maximum flux linkage of

$$\Psi_{max} = NB_g \pi r l \quad \ldots\ldots\ldots\ldots\ldots\ldots (4)$$

If the rotor's position is now considered, the flux linkage is given as a function of position by

$$\Psi(\theta) = (1 - \frac{\theta}{\pi/2})\Psi_{max} \ldots\ldots\ldots\ldots (5)$$

$\Psi(\theta)$ is shown in Figure 9(b) for both coils. From the flux linkage, the instantaneous e.m.f. induced in the coil can be determined in the conventional manner as

$$e = -\frac{d\Psi}{d_t} = -\frac{d\Psi}{d_\theta}\frac{d_\theta}{d_t} = -\omega_m \frac{d\Psi}{d_\theta} \quad \ldots(6)$$

$$e = NB_g \pi r l \omega_m \quad \ldots\ldots (7)$$

where ω_m is the mechanical rotational speed in red s^{-1} To obtain the total back (e.m.f.) for the individual windings, the contribution from both coils needs to be considered; this gives

$$e_p = N_p B_g \pi r l \, \omega_m \ldots\ldots\ldots\ldots\ldots\ldots(8)$$

Where N_p it is equal to 2N for this particular motor.

The phase e.m.f. is shown as a function of the rotor position in Figure 9(c); it is the sum of the voltages for the two windings, which are displaced by 30°,Figure 9(d). In the case of the motor under consideration; the length of constant portion of the e.m.f. waveform is theoretically 150°, but due to the construction of the motor and magnetic fringing, it is in practice closer to 120°.

To control the power to a brushless d.c. motor, a three-phase bridge. Figure 9(a), is used. With the motor star connected, only two phases can carry a current at any one time, and hence only two devices need to conduct in any one switching period. The idealized phase currents are shown in Figure 9(c); they are 120° Wide, with a peak magnitude of I. The switching pattern is arranged to give a current flow against the e.m.f.; a positive current is defined as a motoring current. The device switching sequence in Figure 9(d) is arranged to produce a balanced three-phase motor supply[10].

The torque and the speed constants can be determined by considering the balance between the motor's mechanical output power and its electrical input power over each conduction period; that is

$$P = \omega_m T_e = 2e_p I \quad \ldots\ldots\ldots\ldots\ldots.(9)$$

The factor of two in this equation is the result of the current simultaneously flowing through two motor phases. The electromagnetic torque can be determined from equations (8) and (9)

$$T_e = 4N_p B_g l r I \quad \ldots\ldots\ldots\ldots\ldots (10)$$

Rewriting the voltage and torque equations with, $E = 2e_p$, to represent the e.m.f. of any two phases in series, equations (8) and (10) can be rewritten as

$$E = k\Psi\omega_m \equiv K'_v \, \omega_m \quad \ldots\ldots\ldots\ldots\ldots.(11)$$

$$T_e = k \, \Psi \, I \equiv K'_T \, I \quad \ldots\ldots\ldots\ldots\ldots(12)$$

$$T = I_a K_t \quad \ldots\ldots\ldots\ldots\ldots\ldots\ldots\ldots(13$$

Where the armature constant, $k = 4 \, N_p$, and the flux, $\Psi = B_g \, \pi \, r \, l$,are determined by the construction of the motor. The form of these two equations is very similar to the corresponding equations for brushed d.c. motors (see equation (13)); this explains, to a large extent, why these motors are called BLDCM within the drives industry, when they are more correctly described as permanent-magnet synchronous motors with a trapezoidal flux distribution. In practice, the equations above will only hold good

if the switching between the phases is instantaneous, and if the flux density is uniform with no fringing; while this does not hold true for real motors, these equations can be safely used during the normal selection procedure for a motor and its associated controller [11].

Using the relationships above, the torque-speed characteristics of an ideal d.c. brushless motor can be determined; it is assumed that the commutation and back e.m.f. voltage waveforms are perfect, as shown in Figure 10(a) and Figure10(b). If the star-connected motor configuration is considered, the instantaneous voltage equation can be written as

$$V_s = E + IR \quad \dots\dots\dots\dots \dots (14)$$

Where R is the sum of the individual phase resistances, Vs is the motor's terminal voltage (neglecting semiconductor and other voltage drops), and E is the sum of two phase e.m.f.'s. Using the voltage, torque, and speed equations discussed above, the motor's torque-speed characteristics can be determined. The torque-speed relationship is given by

$$\omega_m = \omega_0 \left(1 - \frac{T}{T_0}\right) \quad \dots\dots\dots\dots.(15)$$
$$\omega_0 = \frac{V_s}{k\Psi} \quad \dots\dots\dots\dots\dots..(16)$$

The stall torque of the motor is given by,
$$T_0 = k\Psi I_0 \quad \dots\dots\dots\dots\dots.(17)$$

Where,

$$I_0 = \frac{V_s}{R} \quad \dots\dots\dots\dots\dots (18)$$

The resultant characteristics, shown in Figure 11, are similar to those for a conventional d.c. motor. The terminal voltage determines the speed of the motor, and under load it will be a function of the winding resistance. As the terminal voltage is modified, the

family of curves shown in Figure 11 will result; in a practical application, terminal-voltage control is normally achieved by the use of pulse-width modulation. As with any other motor, the continuous and intermittent operational limits are determined by the maximum power dissipation of the motor, and the temperature limits imposed by the insulation of the winding.

In contrast to d.c. brushed motors, which have limits imposed by the commutator's operation, the peak torques of brushless motors can be developed to the peak speed, subject to any power-dissipation restrictions. The characteristics will be degraded in real motors by the effects of winding inductance, armature reactance and no uniform flux distribution. [12].

Using the Matlab program to full analysis and calculate the torque of BLDCM, which copied in CD by M-file.

Conclusions

The most important factors in design optimization of BLDC motors are the type of magnet material such as samarium-cobalt or neodymium-iron-boron and it is also critical select the operating point of the magnet by altering magnet arc width.

Choosing operating point of the magnet to be at the maximum energy product of the magnet material will result in minimum magnet volume and cost with better speed versus torque characteristics and high dynamic response.

References
1. M.Rodic, K.Jezernik, A.Sabanovic, "Speed Sensorless Sliding Mode Torque Control of Induction Motor", (Electronics Motors), pages(731–773).,(2000).
2. Paul C. Krause, Oleg Wasynczuk, Scott D. Sudhoff," Analysis of

Electric Machinery and Drive Systems",2nd Edition, page (178), (2001).

3. D. Ishak, Z.Q. Zhu, D. Howe, "Permanent Magnet Brushless Machines with Unequal Tooth Widths and Similar Slot and Pole Numbers", Industry Applications Conference, pages (1055-1061), (2004).

4. Miller, T. J. E.,"Brushless Permanent-Magnet and Reluctance ",Moto. Oxford: Oxford University Press, pages (765-766),(1997).

5. Stratton, J.A., **"Electromagnetic theory"** , EMS- Magnetic Materials and Magnetic Circuit Analysis, New York, pages(7-9) , (1941).

6. John Chiasson, "Modeling and High-performance control of electric machines, Magnetic Fields and Materials", New York, pages(183-186) ,(2004).

7. M.A.Bilewski, A.Fratta, L.Giordano, A.Vagati and F. Villata, "Control of High Performance Interior PM Synchronous Drives", in Conf. Rec. IEEE-IAS Annual Meeting, pages(531–538), (1990).

8. Austin Hughes, "Electric Motors and Drives, Synchronous, Brushless D.C. and Switched Reluctance Drives", Third edition, pages(340-357) ,(2006).

9. Miller, T. J. E, "Brushless Permanent-magnet and Reluctance Motor Drives", Oxford Science Publications, Oxford, UK, pages (169-189), (1989).

10. Hendershot, J. R. and Miller, T. J.E, "Design of Brushless Permanent-Magnet Motors", pages(169-173), (1994).

11. Miller, T. J. E., "Electronic Control of Switched Reluctance Machines", pages(176-178) , (2001).

12. A.E.Fitzgerald ,Electric Machinery, "Speed a nd Torque Control", McGraw-Hill Higher Education, pages(559-562),(2003).
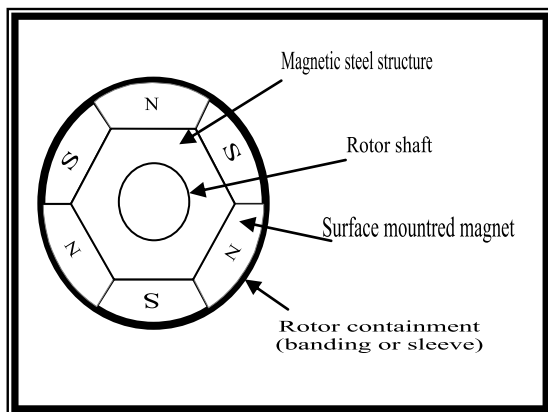
(a)Rotor cross-section of 6- pole BLDC motor with magnet mounted on rotor flash.
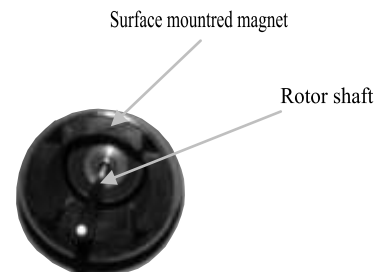
(b)Rotor crossection of 4- pole BLDC motor with magnet mounted on rotor flash.

Figure(1): Rotor cross-section BLDC motor with magnet mounted on cylindrical rotor structure
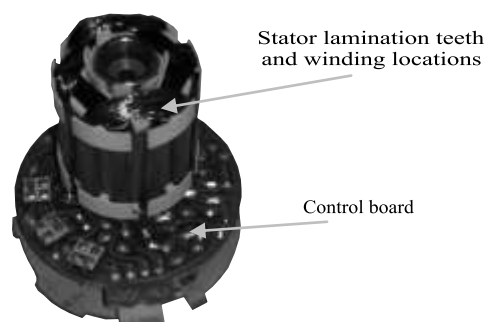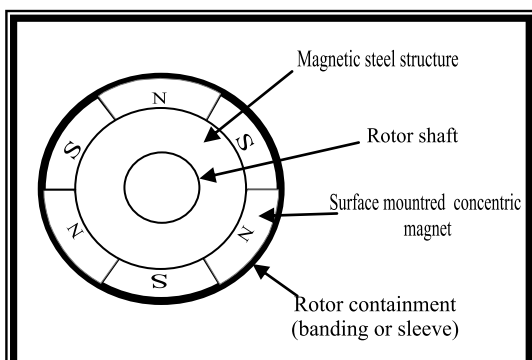
(a)Rotor cross-section of six   pole   BLDC motor with magnet mounted on cylindrical rotor structure.

(b) Stator of 3- pole BLDC motor with electronics board control .

Figure (2): Brushless direct current (dc) motor with magnet mounted on cylindrical rotor structure.
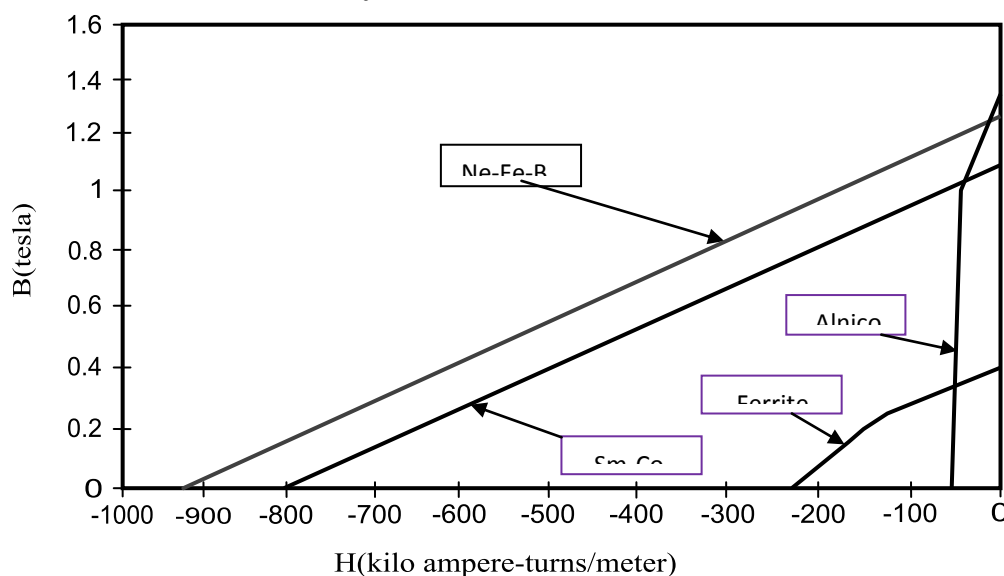

**Figure (3): Typical B-H curves for several magnet types**.
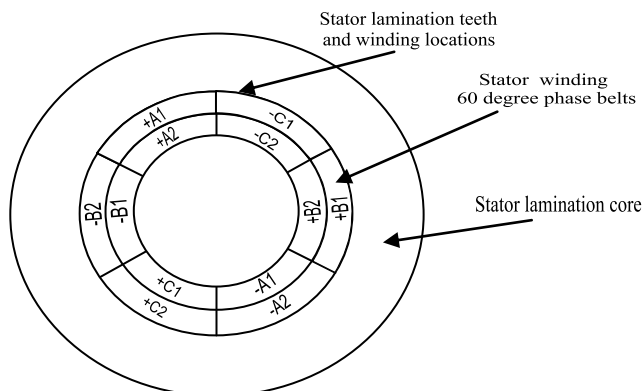
**Figure (4): Phase location for three-phase, two-pole ,full-pitch ,two-layer stator winding.**
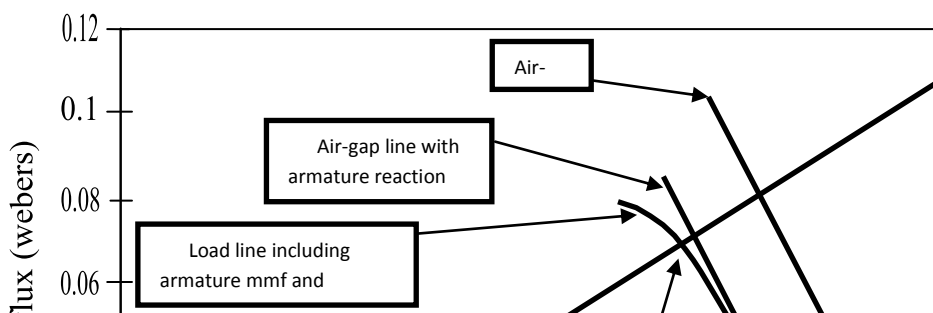
Figure (5): Load line superimposed on magnet characteristics.
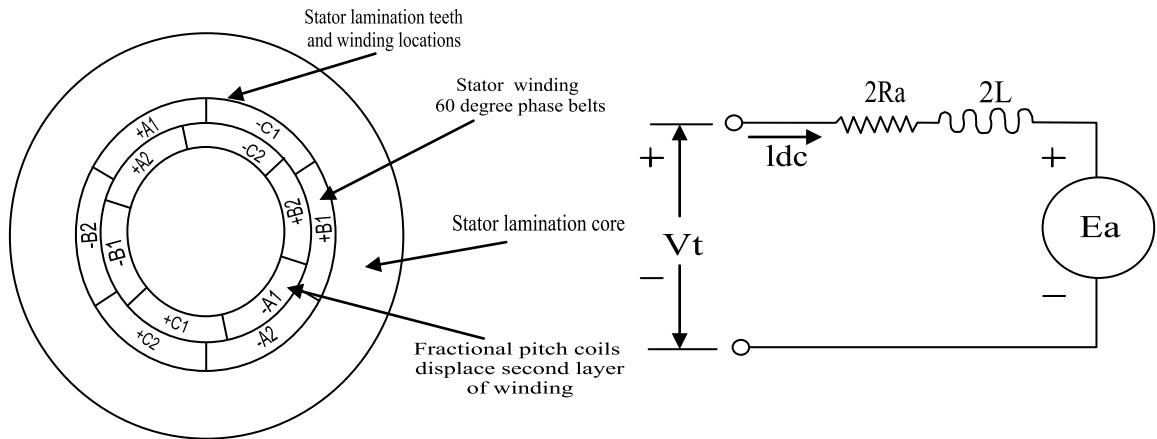
Figure(6): Phase location for three-phase , two-pole ,fractional-pitch ,two-layer stator winding.

Figure (7): BLDC motor equivalent circuit including stator inductance
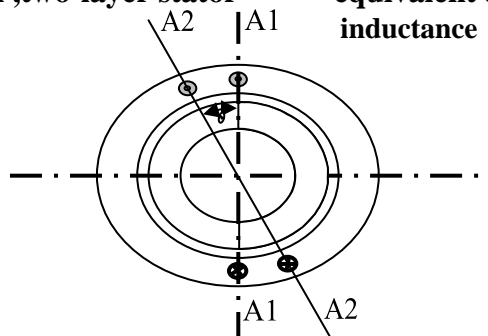
Figure(8): Cross section of idealized brushless motor ,showing two coil for a single phase, $\theta = 30^o$.

phase, $\theta = 30^o$.
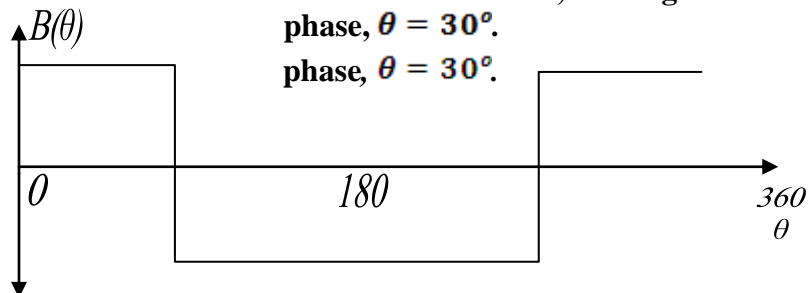
(a)The magnetic flux density in the air-gap, $B(\theta)$
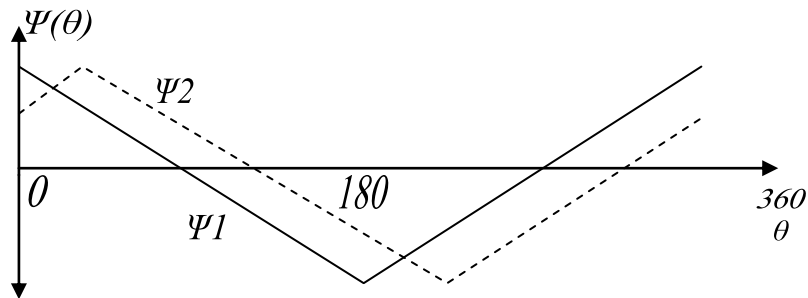
**(b)The magnetic flux linkage in the air-gap, $\Psi(\theta)$**
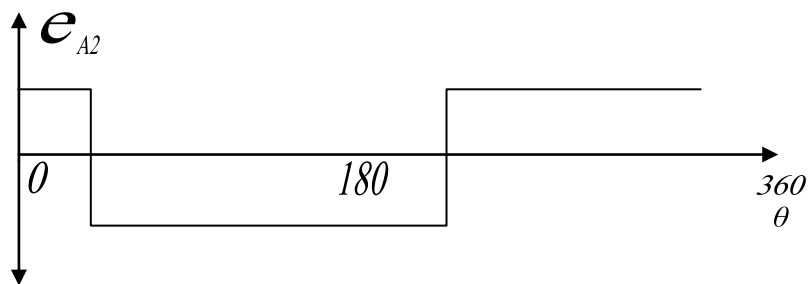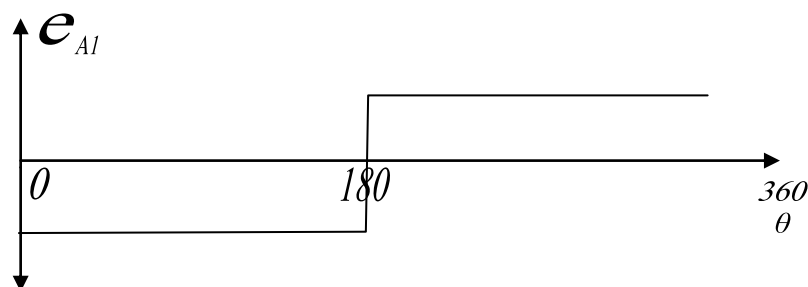
(c)The e.m.f. of the individual coils.
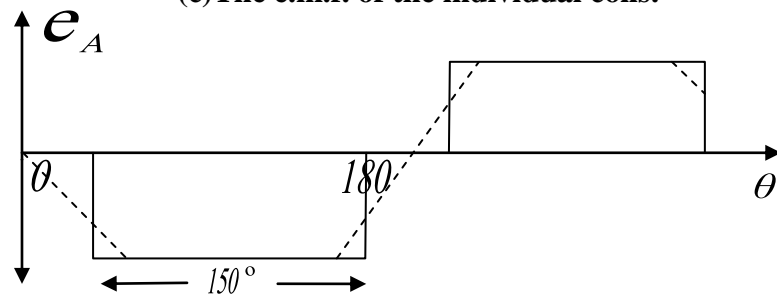
(d)The e.m.f. of a phase.

Figure (9): The waveform for an idealized brushless motor .
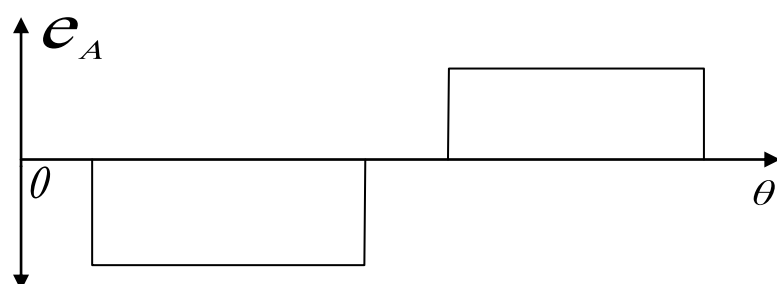
(a)The e.m.f. for phase A as function of position
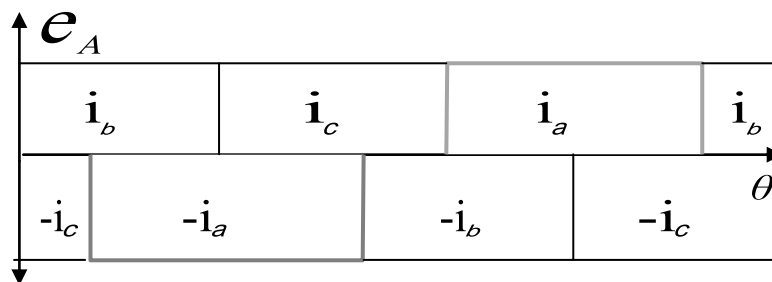
(b)The ideal current pattern for the A phase.

**Figure (10): The switching requirements for an ideal brushless motor.**
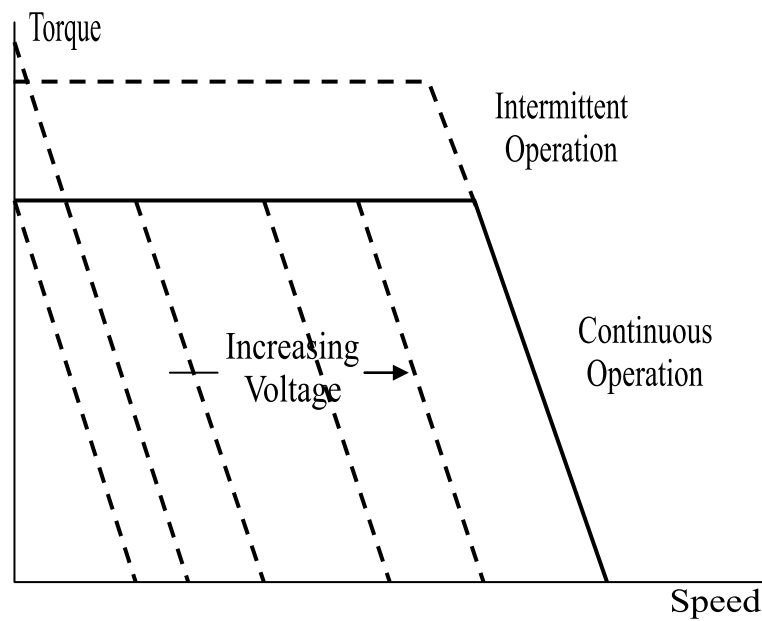
Figure (11): The torque speed characteristics of an ideal brushless d.c. motor